



## A multidating approach applied to historical slackwater flood deposits of the Gardon River, SE France

L. Dezileau, B. Terrier, J.F. Berger, P. Blanchemanche, A. Latapie, R. Freydier, L. Bremond, A. Paquier, M. Lang, J.L. Delgado

### ► To cite this version:

L. Dezileau, B. Terrier, J.F. Berger, P. Blanchemanche, A. Latapie, et al.. A multidating approach applied to historical slackwater flood deposits of the Gardon River, SE France. *Geomorphology*, Elsevier, 2014, 214, p. 56 - p. 68. <hal-01059669>

**HAL Id: hal-01059669**

**<https://hal.archives-ouvertes.fr/hal-01059669>**

Submitted on 1 Sep 2014

**HAL** is a multi-disciplinary open access archive for the deposit and dissemination of scientific research documents, whether they are published or not. The documents may come from teaching and research institutions in France or abroad, or from public or private research centers.

L'archive ouverte pluridisciplinaire **HAL**, est destinée au dépôt et à la diffusion de documents scientifiques de niveau recherche, publiés ou non, émanant des établissements d'enseignement et de recherche français ou étrangers, des laboratoires publics ou privés.

# **A multidating approach applied to historical slackwater flood deposits of the Gardon River, SE France**

L.Dezileau<sup>a,\*</sup>, B.Terrier<sup>b</sup>, J. F.Berger<sup>c</sup>, P.Blanchemanche<sup>d</sup>, A.Latapie<sup>e</sup>,  
R.Freydier<sup>f</sup>, L.Bremond<sup>g</sup>, A.Paquier<sup>e</sup>, M.Lang<sup>e</sup>, J.L.Delgado<sup>h</sup>

<sup>a</sup>Geosciences Montpellier, Université Montpellier 2, CNRS, UMR 5243, France

<sup>b</sup>Agence de l'eau Rhône-Méditerranée et Corse, Lyon cedex, France

<sup>c</sup>Environnement Ville et Société, Université Lumière Lyon 2, CNRS, France

<sup>d</sup>Archéologie des Sociétés Méditerranéennes, CNRS, UMR 5140, France

<sup>e</sup>Irstea, UR HHLy, CS 70077, Villeurbanne, France

<sup>f</sup>Hydrosciences Montpellier, Université Montpellier 2, CNRS, UMR 5569, France

<sup>g</sup>Centre de Bio-Archéologie et d'Ecologie, EPHE, Université Montpellier 2, CNRS, UMR 5059, France

<sup>h</sup>CETE Méditerranée, Aix-en-Provence, France

\* Corresponding author: UMR 5243 CC60 UM2/CNRS, Place E. Bataillon 34095 Montpellier cedex 5, France. Fax:  
+33 (0) 4 67 14 49 30 ;E-mail: [laurent.dezileau@gm.univ-montp2.fr](mailto:laurent.dezileau@gm.univ-montp2.fr).

*Geomorphology*, 214, 56-68, <http://dx.doi.org/10.1016/j.geomorph.2014.03.017>

## 25 **Abstract**

26 A multidating approach was carried out on slackwater flood deposits, preserved in valley side  
27 rock cave and terrace, of the Gardon River in Languedoc, southeast France. Lead-210, caesium-  
28 137, and geochemical analysis of mining-contaminated slackwater flood sediments have been  
29 used to reconstruct the history of these flood deposits. These age controls were combined with  
30 the continuous record of Gardon flow since 1890, and the combined records were then used to  
31 assign ages to slackwater deposits. The stratigraphic records of terrace GE and cave GG were  
32 excellent examples to illustrate the effects of erosion/preservation in a context of a progressively  
33 self-censoring, vertically accreting sequence. The sedimentary flood record of the terrace GE  
34 located at 10 m above the channel bed is complete for years post-1958 but incomplete before.  
35 During the 78-year period 1880-1958, 25 floods of a sufficient magnitude ( $> 1450 \text{ m}^3/\text{s}$ ) have  
36 covered the terrace. Since 1958, however, the frequency of inundation of the deposits has been  
37 lower: only 5 or 6 floods in 52 years have been large enough to exceed the necessary threshold  
38 discharge ( $> 1700 \text{ m}^3/\text{s}$ ). The progressive increase of threshold discharge and the reduced  
39 frequency of inundation at the terrace could allow stabilisation of the vegetation cover and  
40 improved protection against erosion from subsequent large magnitude flood events. The  
41 sedimentary flood record seems complete for cave GG located at 15 m above the channel bed.  
42 Here, the low frequency of events would have enabled a high degree of stabilisation of the  
43 sedimentary flood record, rendering the deposits less susceptible to erosion.

44 Radiocarbon dating are used in this study and compared to the other dating techniques. Eighty  
45 percent of radiocarbon dates on charcoals were considerably older than those obtained by the  
46 other techniques in the terrace. On the other hand, radiocarbon dating on seeds provided better  
47 results. This discrepancy between radiocarbon dates on charcoal and seeds is explained by the

48 nature of the dated material (permanent wood vs. annual production and resistance to degradation  
49 process). Finally, we showed in this study that although the most common dating technique used  
50 in paleoflood hydrology is radiocarbon dating, usually on charcoal preserved within slackwater  
51 flood sediments, this method did not permitus to define a coherent age model. Only the combined  
52 use of lead-210, caesium-137, and geochemical analysis of mining-contaminated sediments with  
53 the instrumental flood record can be applied to discriminate and date the recent slackwater  
54 deposits of the terrace GE and cave GG.

55  
56 *Keywords:* paleoflood hydrology; floods; hydraulic modelling; lead-210; caesium-137; radiocarbon  
57 dating; historical record of mining activity

## 58 **1. Introduction**

59 Palaeoflood hydrology is the reconstruction of the magnitude and frequency of large floods using  
60 geological evidence (Baker et al., 2002). Methods and concepts of paleohydrology have been  
61 described extensively in the literature (e.g., Kochel et al., 1982; Ely and Baker, 1985; Baker,  
62 1987; Benito and Thorndycraft, 2005). Only some of the general concepts are briefly reiterated  
63 here. The methodology combines (i) stratigraphic and sedimentologic analyses to identify the  
64 number of flood units preserved within a particular sedimentary sequence; (ii) hydraulic  
65 modelling to calculate minimum discharge estimates from the known elevations of slackwater  
66 flood sediments; (iii) dating techniques to determine the chronology of flood occurrence; and (iv)  
67 establishment of possible links between past climatic changes and the frequency/magnitude of  
68 flood events. Although the main aim of palaeoflood hydrology is to lengthen the flood series  
69 beyond that of the instrumental record, significant benefits can also be gained by accurately  
70 dating modern slackwater flood deposits (Thorndycraft et al., 2004a,b). As these events occurred

71 during the instrumental period, the potential to correlate the modern sedimentary flood record  
72 with the data measured at gauging stations is possible. This is of particular importance in  
73 understanding the palaeoflood record preserved over centennial timescales (Benito et al., 2004).

74

75 In this study,  $^{14}\text{C}$ ,  $^{210}\text{Pb}$ , and  $^{137}\text{Cs}$  dating and geochemical analyses (Pb and Al concentrations)  
76 were carried out on slackwater flood deposits, preserved in valley side rock cave and terrace, of  
77 the Gardon River in Languedoc in southeast France (Fig. 1). The study sites are located near  
78 Remoulins where a gauging station has been operational over the last 130 years. This provided  
79 the potential for correlation between the instrumental and sedimentary flood records. The two  
80 largest floods of the twentieth and twenty-first centuries, namely the 1958 and 2002 events (with  
81 estimated discharges of  $6400\text{ m}^3/\text{s}$  and  $7200\text{ m}^3/\text{s}$ , respectively, at Remoulins, compared to a  
82 mean annual flow of  $33\text{ m}^3/\text{s}$ ) occurred during the dating range of the  $^{137}\text{Cs}$  and  $^{210}\text{Pb}$  methods,  
83 thereby providing the potential for comparison between these events and palaeofloods. Finally,  
84 our analysis of slackwater flood deposits illustrates important uncertainties related to stratigraphic  
85 studies of paleofloods. These uncertainties bear directly on related limitations in individual event  
86 discrimination and temporal resolution of typical slackwater paleoflood records caused by effects  
87 of erosion/preservation in a context of a progressively self-censoring vertically accreting  
88 sequence.

89

## 90 **2. Dating techniques**

91 Different techniques are available to date recent slackwater deposits.  $^{137}\text{Cs}$  dating has been used  
92 for determining the chronology of modern sediment deposits.  $^{137}\text{Cs}$  is an artificial radionuclide  
93 that was first released into the atmosphere by nuclear bomb testing in the mid-1950s. The

94 temporal patterns of  $^{137}\text{Cs}$  input are characterized by a first peak in 1959 and a second peak at  
95 1962-1964; the termination of  $^{137}\text{Cs}$  input occurred around mid-1980s. Some areas may have had  
96 an additional input in 1986 after the Chernobyl incident.  $^{137}\text{Cs}$  reached the land surface by  
97 atmospheric fallout. The accumulation of  $^{137}\text{Cs}$  in sedimentary deposits throughout the world  
98 therefore began by the early to mid-1950s (e.g., Popp et al., 1988). Analysis of  $^{137}\text{Cs}$  has been  
99 applied to fine-grained deposits to quantify soil erosion and lake sedimentation rates (e.g., Ritchie  
100 et al., 1974; Sutherland, 1989), to date oxbow sedimentation and modern fine-grained floodplain  
101 sediments (Popp et al., 1988; Walling and He, 1997; Bonté et al., 2001; Stokes and Walling,  
102 2003). However,  $^{137}\text{Cs}$  is strongly adsorbed to clay particles and is transported with the  
103 suspended load rather than in solution (McHenry and Ritchie, 1977). The detectable activity of  
104  $^{137}\text{Cs}$  is related to the clay content of the sediments (McHenry and Ritchie, 1977; Popp et al.,  
105 1988), which poses a potential problem when the technique is applied to alluvial deposits with  
106 relatively low clay content. Studies analysing the post-bomb  $^{137}\text{Cs}$  content in modern slackwater  
107 flood deposits from the San Francisco, Paria rivers in Arizona and from the Llobregat River in  
108 Spain (Ely et al., 1992; Thorndycraft et al., 2005b) have shown that the technique can also be  
109 successfully applied to date fluvial sediments characterized by a mix of fine and coarser particles.  
110 The  $^{137}\text{Cs}$  dating results from the Gardon River study reaches can be tested using the combined  
111 data of palaeoflood stratigraphy, discharge estimation by hydraulic modelling and the  
112 instrumental discharge record.

113  
114 The basic methodology of  $^{210}\text{Pb}$  dating was established in a seminal paper by Golberg (1963).  
115  $^{210}\text{Pb}$  precipitates from the atmosphere through  $^{222}\text{Rn}$  decay and accumulates in surface soils,  
116 glaciers, or lakes where successive layers of material are buried by later deposits.  $^{210}\text{Pb}$   
117 deposition on land is primarily owing to meteoric fallout; and it is adsorbed quickly and

118 tenaciously by the surfaces of fine sediments, primarily onto clays, where, even more so than  
119  $^{137}\text{Cs}$ , it is chemically immobile (Cremers et al., 1988). There it undergoes beta decay to  $^{210}\text{Bi}$   
120 with a half-life of 22.3 years.  $^{210}\text{Pb}$  fallout is generally found to be constant at any given location  
121 over time scales relevant to  $^{210}\text{Pb}$  geochronology (Appleby and Oldfield, 1978, 1992; He and  
122 Walling, 1996). In the simplest model, the initial  $(^{210}\text{Pb})_{\text{ex}}$  is assumed constant and thus  $(^{210}\text{Pb})_{\text{ex}}$  at  
123 any time is given by the radioactive decay law. The sedimentation rates in slackwater flood  
124 deposits are clearly variable and discontinuous because of the near-instantaneous sedimentation  
125 of flood deposits so that this type of model is difficult to use (He and Walling, 1996; Aalto and  
126 Nittrouer, 2012). However, this technique can be successfully applied to assess whether an  
127 apparent accumulation of 'fresh sediment' exists (<100 years, i.e., ~4 to 5 times its decay period of  
128 22.3 years).  $^{210}\text{Pb}$  dating will be tested in the Gardon River.

129  
130 Carbon-14 analysis is the standard technique for dating Holocene alluvial deposits. Radiocarbon  
131 dating of slackwater flood sediments has an applicable age range of between ca. 300 and 55,000  
132 yBP (Trumbore, 2000) and therefore cannot accurately date the sediments of flood events from  
133 the most recent centuries. With atmospheric testing of nuclear weapons after 1950,  $^{14}\text{C}$  activity in  
134 the troposphere rapidly increased, reaching a peak of 100% above normal in the early 1960s  
135 (Nydal and Lovseth, 1983). For post-bomb alluvial deposits, radiocarbon dating on organic  
136 materials preserved within slackwater flood sediments gives a 'modern age' that can be useful to  
137 assess whether an apparent accumulation of "fresh sediment" exists in the study area. The  $^{14}\text{C}$  age  
138 of organic materials entrained in an alluvial deposit may differ significantly from the actual age  
139 of the deposit, depending on the residence time of the organics within the environment (Ely et al.,  
140 1992). Thus, for flood deposits, the type of organic material available constrains the accuracy of  
141 the resulting dates. In particular, detrital wood and charcoal can predate fluvial deposits by

142 several hundred years (Atwater et al., 1990). The radiocarbon dating is not the best technique to  
143 accurately date the sediments of flood events from the most recent centuries (Trumbore, 2000)  
144 but was used in this study to be tested by obtaining radiocarbon dates for several types of plant  
145 materials from well-dated flood deposits.

146  
147 Ages for modern flood deposits can be correctly assigned with the use of trace metals generated  
148 by mining activity. This geochemical analysis of mining-contaminated floodplain sediments has  
149 been used to date floodplain sediment and slackwater flood deposits where a known historical  
150 record of mining within the catchment exists (e.g., Davies and Lewin, 1974; Lewin et al., 1977;  
151 Hindel et al., 1996; Knox and Daniels, 2002; Thorndycraft et al., 2004a,b). The extraction of Zn–  
152 Pb from the Gardon River basin started in 1730 (Elbaz-Poulichet et al., 2006). The number of  
153 mining concessions increased significantly between 1860 and 1930. During this period, mining  
154 activity generated 400,000 tons of tailings. Between 1951 and 1963, Pennaroya and then  
155 Metaleurop mining companies extensively exploited the ore generating between 2,300,000 and  
156 5,000,000 tons of tailings (30,000 tons of lead and 3500 tons of Zn). This mining activity ceased  
157 in 1993. One of the most important mines on the Gardon River basin is the Carnoules mine,  
158 which has generated a total of 1,500,000 tons of wastes. The mine officially closed on 24  
159 October 1963. In September 1976, the tailings partially collapsed caused by a violent  
160 Mediterranean thunderstorm. This was followed in October 1976 by the sudden evacuation of the  
161 100,000 m<sup>3</sup> of water initially contained in a lake that had formed in the tailing stock. The accident  
162 was responsible for a major pollution of water and soil in the Gardon River basin (DREAL,  
163 2008). This paper describes a combined stratigraphic and geochemical approach to identify traces  
164 of historic tin mining activity within slackwater deposits of the Gardon River.

165



### 166 **3. Gardon River basin flood hydrology**

#### 167 *3.1. Study area description*

168 The Gardon River watershed (1858 km<sup>2</sup> at Remoulins) is located in the southeast Massif Central  
169 mountains and is ~ 135 km long from its headwaters at 1699 m above sea level (Mount Lozere)  
170 to its confluence with the Rhône River at 6 m asl (Fig. 1A). The Gardon is the southern most  
171 tributary of the Rhône River. In terms of geology (Fig. 1B), the Cévennes Mountains are mainly  
172 composed of Paleozoic granite, schist, gneiss, and sandstone (Bonnifait et al., 2009). The rivers  
173 present a high degree of sinuosity in this upstream area. Farther downstream, the Gardon River  
174 crosses the Gard plains, which are based on Mesozoic carbonate formations with a stratigraphical  
175 series ranging from Jurassic (west) to Cretaceous (east). Close to the Cévennes Mountains, this  
176 secondary series is interrupted by a network of NE–SW faults that delineate the Alès graben, a  
177 1500-m graben filled with Tertiary sediments from the Oligocene period. The river then crosses  
178 Cretaceous limestone following deep canyons (the Gardon gorges). These limestone formations  
179 present a high degree of karstification. Downstream, the Mesozoic formations are covered with  
180 the Quaternary sediments of the Rhône River (Bonnifait et al., 2009). The high watershed of the  
181 Gardon River was reforested during the nineteenth century by calcic or acidophile medio-european  
182 beech species, white oak species, *Castanea sativa* forests, and shrublands with *Juniperus*  
183 *communis*. The limestone tableland of Nîmes garrigue, mainly occupied by forests of green oaks  
184 (*Quercus ilex* and *Quercus rotundifolia*), some white oak coppice, a mosaic of a substeppic  
185 grassland with annual grasses from the *Thero-brachypodietea*. The Matorral tree with  
186 *Juniperus phoenicea* occupies the rocky ledges of the limestone tableland, while on the rocky  
187 slopes develop xero-thermophilic formations with *Buxus sempervirens*. The limestone  
188 canyon includes riparian vegetation composed mainly of *Salix alba*, *Populus alba*, and *Fraxinus*

189 *excelsior*, with some pines (*Aleppo* and *Pinion pines*) on pediments and upper alluvial terraces.

190

191 *Insert Fig. 1 near here*

192

193 The study sites are located in the middle reach of the Gardon River in the Cretaceous bedrock  
194 gorge, between Russan and Remoulins. Little to no changes in the shape of the canyon occurred  
195 throughout the late Holocene. The identification of flood sediment sources transported into the  
196 gorge is facilitated by the strong contrast between the granitic, basaltic, and metamorphic bedrock  
197 of the upper catchment and the carbonates of the Gardon gorge. Slackwater flood sediments have  
198 been deposited and preserved on high-standing terraces along channel margins and in many  
199 karstic caves and alcoves.

200

201

### 202 *3.2. Flood hydrology and hydroclimatology*

203 The Gardon River has a typically Mediterranean regime with a low mean annual discharge (33  
204 m<sup>3</sup>/s, SAGE des Gardons, 2000), extreme seasonal variations, and flood peaks around 100 times  
205 greater than the mean discharge. Mean annual rainfall in the catchment varies from 500 to 1100  
206 mm. Nuissier et al. (2008) provided a detailed analysis of typical flash flood events in this region.  
207 Large amounts of precipitation can accumulate over several days, particularly at the end of  
208 summer and beginning of autumn, as frontal disturbances slow down and are reinforced by the  
209 relief of the Massif Central. When a Mesoscale Convective System remains quasistationary for  
210 several hours, heavy rainfall of over 200 mm can be recorded in less than a day and can therefore  
211 lead to devastating flash floods.

212 A large set of hydrological data is available from the flood forecasting service (known as the  
213 ‘Service de Prevision des Crues’ or SPC30) and the local authority (‘Smage des Gardons’). The  
214 gauging station located at Remoulins (~15 km downstream of study sites) provides stage  
215 observations from 1890 onward (Fig.2). Since 1890, three major flood events have been recorded  
216 with water levels > 7 m and estimated peak flood discharges defined from the stage-discharge  
217 relationship > 5000 m<sup>3</sup>/s, namely the 16-17 October 1907 (5300 m<sup>3</sup>/s), 4 October 1958 (6400  
218 m<sup>3</sup>/s), and 8-9 September 2002 (7000 m<sup>3</sup>/s) floods. This last extreme flood event claimed the  
219 lives of 23 people and caused €1.2 billion worth of damage to towns and villages along the river.  
220 Seven thousand houses were damaged, 100 of which were completely destroyed and 1500  
221 submerged under 2 m of water (Huet et al., 2003).

222

223  
224

*Insert Fig. 2 near here*

### 225 *3.3. Previous paleoflood studies of the Gardon River*

226 One paleoflood study of the Gardon River has been conducted just downstream of our study area  
227 (Sheffer et al., 2008). The main objectives of their study were (i) to provide an accurate and  
228 reliable discharge estimation of the 2002 flood at the study reach, (ii) to reconstruct a record of  
229 major flood events using paleoflood hydrology, and (iii) to improve the understanding of the  
230 2002flood magnitude and consider the long-term perspective of rare events and extreme flood  
231 discharges provided by the paleoflood record. They concluded that according to slackwater  
232 deposits found at different sites at least five extreme events occurred during the Little Ice Age.  
233 Each was larger than the 2002 flood (Sheffer et al., 2008).

234

235

## 236 **4. Methods**

### 237 *4.1. Paleoflood analysis*

238  
239 During large floods in canyons, slackwater deposits(usually fine sands and silts) accumulate  
240 relatively rapidly from suspension in sites of abrupt drop in flow velocity (Ely and Baker, 1985;  
241 Kochel and Baker, 1988; Benito et al., 2003a). As a result, a layer of these deposits is formed.  
242 This sediment may be preserved in protected sites, such as caves and alcoves in the canyon walls,  
243 and backwater zones behind valley constrictions (Kochel et al., 1982; Ely and Baker, 1985; Baker  
244 and Kochel, 1988; Enzel et al., 1994; Springer, 2002; Webb and Jarrett, 2002; Benito et al.,  
245 2003b; Benito and Thorndycraft, 2005). Subsequent flood deposits may accumulate above this  
246 layer by floods with stages higher than the top of the depositional sequence (Baker, 1987).

247  
248 For this study, two depositional sequences (Fig. 3) were investigated along the Gardon River in a  
249 high-standing, terrace-like bench of aggrading sediments (GE located at 10 m above the channel  
250 bed, the base of the terrace is at 2 m, the terrace is 70 m wide and 300 m long) and in a cave (GG  
251 at 15 m above the channel bed). Sites of slackwater flood sediment deposition were identified  
252 along the study reaches, and sections were cut to expose the sedimentary sequences. Individual  
253 flood units were determined through a close inspection of depositional breaks and/or indicators of  
254 surficial exposure (e.g., presence of a paleosol, clay layers at the top of a unit, detection of  
255 erosional surfaces, bioturbation features, angular clast layers deposits in local alcoves or slope  
256 material accumulation between flood events, fireplaces, and anthropogenic occupation layers  
257 between flood events).

258 *Insert Fig. 3 near here*

259

260 4.2. Analytical methods  
261

262 Dating of sedimentary layers was carried out using  $^{210}\text{Pb}$  and  $^{137}\text{Cs}$  methods on a centennial  
263 timescale. Both nuclides together with U, Th, and  $^{226}\text{Ra}$  were determined by gamma spectrometry  
264 at the Géosciences Montpellier Laboratory. The 1-cm-thick sediment layers were sieved in order  
265 to obtain the fraction smaller than 1 mm. This material was then finely crushed after drying and  
266 transferred into small gas-tight PETP (polyethylene terephthalate) tubes (internal height and  
267 diameter of 38 and 14 mm, respectively), and stored for more than 3 weeks to ensure equilibrium  
268 between  $^{226}\text{Ra}$  and  $^{222}\text{Rn}$ . The activities of the nuclides of interest were determined using a  
269 Canberra Ge well detector and compared with the known activities of an in-house standard.  
270 Activities of  $^{210}\text{Pb}$  were determined by integrating the area of the 46.5-keV photo-peak.  $^{226}\text{Ra}$   
271 activities were determined from the average of values derived from the 186.2-keV peak of  $^{226}\text{Ra}$   
272 and the peaks of its progeny in secular equilibrium with  $^{214}\text{Pb}$  (295 and 352 keV) and  $^{214}\text{Bi}$  (609  
273 keV). In each sample, the ( $^{210}\text{Pb}$  unsupported) excess activities were calculated by subtracting the  
274 ( $^{226}\text{Ra}$  supported) activity from the total ( $^{210}\text{Pb}$ ) activity. Note that, throughout this paper,  
275 parentheses () denote activities. Activities of  $^{137}\text{Cs}$  were determined by integrating the area of the  
276 661-keV photo-peak. Error bars on ( $^{210}\text{Pbex}$ ) and ( $^{137}\text{Cs}$ ) do not exceed 6%.

277 The  $^{14}\text{C}$  analyses were conducted at the Laboratoire de Mesure  $^{14}\text{C}$  (LMC14) on the ARTEMIS  
278 accelerator mass spectrometer in the CEA Institute at Saclay (Atomic Energy Commission).  
279 These  $^{14}\text{C}$  analyses were carried out with the standard procedures described by Tisnérat-Laborde  
280 et al. (2001). The  $^{14}\text{C}$  ages were converted to calendar years using the CALIB 6.1.0 calibration  
281 program (Stuiver and Reimer, 1993). A summary of the samples submitted for dating, and their  
282 associated results, is presented in Table 1. All radiocarbon dates are quoted in the text as the  $2\sigma$   
283 calibrated age range.

284

285

*Insert Table 1 near here*

286

287

288 Before analysis, sediment samples were ground in an agate mortar and digested in a Teflon beaker  
289 on a hot plate. One hundred milligrams of sediment were digested using a three step procedure:  
290 1/H<sub>2</sub>O<sub>2</sub>, 2/HF:HNO<sub>3</sub>:HClO<sub>4</sub>, and 3/HNO<sub>3</sub>:HCl. The Al and Pb concentrations were determined  
291 using an ICP-MS, X Series II (Thermo Fisher Scientific), equipped with a CCT (Collision Cell  
292 Technology) chamber at the Hydrosiences Montpellier Laboratory. Certified reference material  
293 from LGC Standards, i.e., LGC6189 (river sediment), was used to check analytical accuracy and  
294 precision. Measured concentrations agree with recommended values to within 10% (Al) and 3%  
295 (Pb). To find out if there was an enrichment of lead relative to the local baseline, an enrichment  
296 factor (EF) technique was used. The enrichment factor (EF) of lead is calculated following the  
297 equation:  $EF_{Pb} = (Pb/Al)_{sample} / (Pb/Al)_{Average\ Local\ Background}$ .

298 The  $(Pb/Fe)_{sample}$  is the ratio of Pb and Fe concentration of the sample and  $(Pb/Fe)_{Average\ Local}$   
299  $background$  is the ratio of Pb and Fe concentration of a background. The background concentrations  
300 of Pb were taken from the base of the terrace (i.e., pre-industrial period concentrations).  
301 Grainsize analysis was conducted on contiguous 1 cm samples using a Beckman-Coulter  
302 LS13320 laser diffraction particlesize analyser at the Géosciences Montpellier Laboratory. Grain  
303 size distribution measurements were made on the < 1 mm sediment fraction.

304

305 *4.3. Hydraulic modelling*

306 *4.3.1. Model description*

307 A one-dimensional (1D) hydraulic model of the Gorges was built using RubarBE, a numerical  
308 model that solves the shallow water equations and uses an explicit second-order Godunov-type  
309 scheme (El kadi Abderrezzak and Paquier, 2009). The modelled reach is ~31.5 km long and  
310 extends from Russan, located at the entrance of the Gorges, to downstream of the Remoulins  
311 gauging station, located at the exit of the Gorges. Topographic data were obtained from the  
312 SPC30 and the Smage des Gardons. In addition, two surveying campaigns were carried out in the  
313 Gorges in order to obtain detailed topographic data near the paleoflood sites. During these  
314 campaigns, 21 profiles were surveyed with a Leica TC 305 total station and a differential GPS  
315 Leica 1200 with GPS-GLONASS receptor. In total, 95 profiles were used to construct the  
316 hydraulic model. The 2002 flood hydrographs provided by the SPC30 at Russan and Remoulins  
317 gauging stations revealed that the peak flows were approximately the same at both locations. In  
318 order to simulate past flood events, it was therefore decided that the flow at Remoulins be used as  
319 an upstream boundary condition at Russan. The downstream boundary condition has been  
320 defined with the water levels available at the Remoulins gauging station.

321 A sensitivity analysis has been conducted to assess the influence of the Alzon River, a tributary  
322 draining an area of 203 km<sup>2</sup>, on the water levels calculated at the paleoflood sites.

323

#### 324 *4.3.2. Model calibration*

325 Following the 2002 flood event, a post-event analysis of debris lines and observed water levels  
326 was conducted by the Smage des Gardons. The model was thus calibrated on the 21 water levels  
327 available for the 2002 event and validated on the 10 water levels recorded for the 1958 event. On  
328 average, the difference between the measured water levels and the results of the model is -0.11 m  
329 with a standard deviation of 0.69 m for the 2002 flood event. For the 1958 event, the average  
330 difference is -0.95 m with a standard deviation of 0.94 m. Most of the debris lines surveyed are

331 located in the vicinity of hydraulic singularities such as bridges. The flow behaviour in these  
332 areas is notably difficult to reproduce in a 1D hydraulic model. Furthermore, the levels of the  
333 debris lines in the vicinity of the bridge may not be representative of the highest mean water level  
334 and may be the result of water surface fluctuations that cannot be reproduced by the 1D model.  
335 The results of the calibration are therefore regarded as satisfactory.

336

337 *Insert Fig. 4 near here*

338

#### 339 *4.3.2. Sensitivity analysis*

340 The results of the model with the varying roughness coefficient allow the determination of an  
341 envelope of stage discharge relationship at the two paleoflood sites (Fig. 4B). The sensitivity  
342 analysis on the flow record used as an upstream boundary condition in the model also provides an  
343 envelope on the water levels and discharges at the paleosites for each flood event. Results are  
344 then compared with the historical flood records available at Remoulins to identify the events that  
345 may have reached or submerged the sites (Fig.4C). Envelopes at the paleoflood sites are bound  
346 by the scenarios of the sensitivity analysis of  $Q \pm 10\%$  combined with the scenarios of  $K_s \pm 10\%$ .  
347 These results can be put into perspective with the dating approach and are discussed in the  
348 following paragraphs.

349

## 350 **5. Results**

### 351 *5.1. Stratigraphic records of flood events in terrace GE and cave GG*

#### 352 *5.1.1. Terrace GE*

353 At terrace GE, the stratigraphy consists of 20 individual slackwater flood units. Based on the



354 results of the hydraulic model (stage-discharge curve), a flood event of intensity similar to that of  
355 the 1972 event ( $\sim 2100 \text{ m}^3/\text{s}$  at Remoulins) is required for a flood event to cover the uppermost  
356 flood unit of the terrace. Figure 5 presents  $^{210}\text{Pb}_{\text{ex}}$  and  $^{137}\text{Cs}$  activities and the enrichment factor  
357 of Pb for this terrace. Also illustrated is the minimum discharge estimate calculated for the  
358 floodwaters to cover the terrace during flood events.

359 The  $^{137}\text{Cs}$  activity is recorded in flood units GE17, GE18, GE19, and GE20, with maximum  
360 values of 38 and 45 mBq/g in units GE17 and GE18, respectively (Fig.5). No  $^{137}\text{Cs}$  is found in  
361 the older deposits of the profile. The first post-1955 event, identified by the first trace of  $^{137}\text{Cs}$   
362 activity in the profile, is that of GE17 indicating that the four flood deposits GE17-GE20 all post-  
363 date this period. More particularly, the high  $^{137}\text{Cs}$  activity recorded in flood units GE17 and  
364 GE18 (38 and 45 mBq/g) can be associated to the maximum atmospheric production in the mid-  
365 1960s (around 1963, Fig. 5).

366 The first flood unit containing  $^{210}\text{Pb}_{\text{ex}}$  activity is unit GE15 located at 90 cm depth in the  
367 stratigraphic profile, with a value of 5 mBq/g. The  $^{210}\text{Pb}_{\text{ex}}$  activity is recorded in flood units GE15,  
368 GE17, GE18, GE19, and GE20, with a maximum value of 58 mBq/g in unit GE19. There is an  
369 apparent accumulation of 'fresh sediment' ( $< 100$  years, i.e., approximately 4 to 5 times the  
370 decay period of  $^{210}\text{Pb}$ ) in the uppermost part of the terrace GE. The  $^{210}\text{Pb}_{\text{ex}}$  can help us to confirm  
371 a number of results produced using  $^{137}\text{Cs}$  dating technique. The high  $^{210}\text{Pb}_{\text{ex}}$  activity recorded in  
372 flood units GE19 and its exponential decrease in the other flood deposits (GE18 to G15) suggests  
373 that the uppermost part of the terrace can be considered as being stratifically undisturbed. In  
374 particular, the first trace of  $^{210}\text{Pb}_{\text{ex}}$  activity in the profile is that of GE15, thereby indicating that  
375 the six flood deposits GE15-GE20 are recent and all post-date approximately the end-1910s (Fig.  
376 7).

377 The geochemistry of the profile shows that enrichment factor (EF) of Pb, with a range of 1.0 to  
378 10.5, exhibits very high variation between the base and the top of the terrace (Fig. 5). The lowest  
379 EF values of Pb (around 1.0) occur in flood units between GE1 and GE9. The EF is higher in the  
380 uppermost flood units of the terrace, around 1.9 between GE10 and GE17, 3.3 in GE18, 10.5 in  
381 GE19, while it decreases in the last flood unit GE20 (3). At 155 cm depth, an increase in the EF  
382 of Pb occurs from a background value of 1.0 (GE9) to a value of 1.9 (GE11). The increase  
383 production of Pb between 1870 and 1905 could explain these increased levels of heavy metals  
384 (Fig 5). In terms of the relative chronology, therefore, the geochemical analysis shows that the  
385 lower stratigraphic slackwater deposits units (GE1 to GE9) are probably older than 1870. The EF  
386 of Pb is higher in the uppermost flood units of the terrace, around 3.3 in GE18 and 10.5 in GE19.  
387 The first high EF of 3.3 can be linked to the strong increase of Pb production during the mid-  
388 1960s (GE18) and the very high EF of 10.5 to the major pollution of the basin in 1976 (GE19,  
389 Fig. 5).

390  
391 In addition to the trace metal,  $^{137}\text{Cs}$  and  $^{210}\text{Pb}_{\text{ex}}$  activities as age marker horizons, extreme floods  
392 during the last 50 years also produced very prominent stratigraphic horizon. These age controls  
393 were combined with the continuous record of stage available from 1890 at the Remoulins  
394 gauging station located 15 km downstream (data from SPC 30). The combined records were then  
395 used to assign ages to slackwater deposits indicative of other large floods in the GE sequence  
396 (Fig 5). The 1958 event, the second largest in instrumental record ( $6400 \text{ m}^3/\text{s}$ ), deposited a 25-  
397 cm- thick unit of medium sands (GE16:  $270 \mu\text{m}$ ). The next three flood units (GE17, GE18, and  
398 GE19) are well marked by the pollution of Pb and  $^{137}\text{Cs}$  and have been assigned to three lower  
399 magnitude floods ( $4000$ ,  $2900$ , and  $3000 \text{ m}^3/\text{s}$ , respectively) that occurred in 1963, 1969, and

400 1976, respectively (Fig. 5). Thin sedimentary layers and fine sands characterize these three flood  
401 units. The 2002 event, the largest in the instrumental record, deposited a 30-cm- thick unit of  
402 medium sands (GE20). From these different flood units, a positive correlation ( $r^2=0.96$ ) exists  
403 between the magnitude of the flood versus the grain size/thickness of the different units. The  
404 sedimentary flood record prior to 1958 at site GE seems incomplete, as indicated by the fact that  
405 fewer post-pollution flood units are preserved (seven units since 1890) than there were flood  
406 events with a discharge of sufficient magnitude to cover the sedimentary surface (Fig. 5). Based  
407 on the results of the hydraulic model, about 25 flood events would have submerged terrace GE  
408 between 1870 ( $>1430 \text{ m}^3/\text{s}$ ) and 1958 ( $>1700 \text{ m}^3/\text{s}$ ) for the scenario for a roughness coefficients  
409  $K$  increased by 10% and input flows overestimated by 10% (Figs. 4C and 5). Assuming that a  
410 minimum depth of water is required above the site in order for the sediment to deposit in a  
411 sufficiently thick layer, it is possible that events of lower magnitudes are not recorded in the  
412 sedimentary record. In that case, based on the possible relationship between sediment grain size  
413 and magnitude, GE15 could be associated to 1951, GE14 to 1943, GE13 to 1933, GE12 to 1915,  
414 GE11 to 1907, GE10 to 1900, and GE9 to 1890 (Fig. 5). Erosion, errors in hydrological  
415 documentary sources, and model approximation could also be at the origin of this low correlation  
416 between sedimentary flood record and the continuous record of Gardon flow between 1890 and  
417 1958.

418

419 *Insert Fig. 5 near here*

420

#### 421 5.1.2. Cave GG

422 Cave GG is located at 15 m above the channel bed with a minimum estimated discharge of  
423 approximately  $4500 \text{ m}^3/\text{s}$  required for floodwaters to reach the site (Fig. 4c). Results from the

424 hydraulic model suggest that at least three events have submerged GG. Cave GG contains more  
425 than 1.5 m of slackwater flood sediments. In this article, only the upper 35 cm will be discussed.  
426 Six depositional units were found on the first 35 cm, four of which correspond to flood deposits  
427 (Fig.6). The flood deposits consist of fine sand to silt, featuring diffused lamination, with many  
428 charcoal pieces and ash lens. Median grain size (d50) is clearly affected by the presence of  
429 charcoals and ash lens. The  $^{137}\text{Cs}$  data indicates activity in only one sample analysed in the upper  
430 part of the profile (GG4 with a value of 2 mBq/g). The same pattern is observed for  $^{210}\text{Pb}_{\text{ex}}$   
431 activity (Fig. 6).  $^{210}\text{Pb}$  activity is recorded in the flood unit GG4 (14mBq/g), with no activity in  
432 the older deposits. The presence of  $^{137}\text{Cs}$  activity and  $^{210}\text{Pb}_{\text{ex}}$  activity in this unit means that the  
433 age of GG4 post-date 1955 (Fig. 6). At 15 cm depth, a slight increase in the EF of lead occurs  
434 (from a background value of 1 to a value of 1.4). The increase production of lead between 1870  
435 and 1905 could explain this increased level of heavy metals occurring in the slackwater deposit  
436 GG2 (Fig 6). The EF of lead is higher in the uppermost flood units of the terrace, around 2.2 in  
437 GG3 and 4.4 in GG4. The high EF of 2.2 and more in this unit means that the age of GG3 and  
438 GG4 post-date the beginning of the twentieth century but cannot be associated to precise  
439 ages. The combined records were then used to assign ages to slackwater deposits indicative of  
440 other large floods in the GG sequence (Fig. 6). The 1907 event, the third largest in instrumental  
441 record (5200 m<sup>3</sup>/s), deposited a 5-cm- thick unit of fine sands (GG2). The next flood unit,  
442 assigned to the second largest in instrumental record (1958:6300 m<sup>3</sup>/s), deposited a 5-cm- thick  
443 unit of fine sands (GG3). The 2002 event, that is the largest in the instrumental record, deposited  
444 a 4-cm- thick unit of fine sands (GG4). The 1961 and 1976 events did not reach the cave and may  
445 explain why the EF of Pb is not higher than 4.4.

446

447

*Insert Fig. 6 near here*

448  
449 *5.2. Radiocarbon dating*  
450 In the fluvial terrace GE, 17 dates were obtained using conventional radiocarbon analysis on  
451 wood charcoals and seeds. All of the obtained dates are plotted in Fig. 7 in yBP (corrected for  
452 isotopic fractionation) and calibrated to calendar years. From this recent terrace GE, one would  
453 normally expect progressively younger dates in the uppermost flood units of the terrace. For  
454 radiocarbon analysis on charcoals, at the exception of the first two radiocarbon dates in GE1 (200  
455 yBP) and GE2 (285 yBP), radiocarbon dates are older than expected for the basal part of the  
456 terrace GE but considerably older (between 520 and 6540 yBP) than those obtained by the other  
457 techniques in the uppermost flood units of the terrace. Uncalibrated  $^{14}\text{C}$  ages of seeds are often in  
458 an inverted stratigraphic position. However, when these ages are calibrated at  $2\sigma$  they are  
459 consistent with those obtained by the other dating techniques.

460

461 *Insert Fig. 7 near here*

462

463

## 464 **6. Discussion**

465

### 466 *6.1. Dating techniques*

467

468 Ages for modern flood deposits have been correctly assigned with the use of  $^{137}\text{Cs}$ . The presence  
469 or absence of  $^{137}\text{Cs}$  in these flood deposits of the Gardon River is not controlled by the particle  
470 size distribution. In the upper four deposits (units 17 through 20),  $^{137}\text{Cs}$  was detected even in the

471 sample with the lowest clay content ( $F < 2\mu\text{m}: 0.03\%$ ) (Fig. 5). Moreover, the uppermost pre-bomb  
472 deposit (unit 15) showed no  $^{137}\text{Cs}$  activity. There was no leaching of  $^{137}\text{Cs}$  into the post-bomb  
473 deposits from the overlying post-bomb deposits, as no samples below unit 16 showed detectable  
474  $^{137}\text{Cs}$ . Four samples from the flood deposit G20 (2002) showed  $^{137}\text{Cs}$  activity, although  
475 atmospheric  $^{137}\text{Cs}$  fallout is negligible during this period. The presence of  $^{137}\text{Cs}$  in this recent  
476 flood deposit could have resulted from the erosion and redeposition of post-1950 floodplain or  
477 terrace deposits. Our results are consistent with other authors (Ely et al., 1992; Thorndycraft et  
478 al., 2005a,b), who found that (i)  $^{137}\text{Cs}$  is concentrated by erosion and redeposition of fine-grained  
479 sediments and (ii) significant  $^{137}\text{Cs}$  activity in sandy sediments indicates that high clay content is  
480 not necessary for this method to be effective in distinguishing pre- and post-1950 deposits.

481 The  $^{210}\text{Pb}_{\text{ex}}$  confirms a number of results produced using the  $^{137}\text{Cs}$  dating technique. The high  
482  $^{210}\text{Pb}_{\text{ex}}$  activity recorded in flood units GE19 and its exponential decrease in the other flood  
483 deposits (GE18 to G15) suggests that the uppermost part of the terrace is recent ( $< 100$  years,  
484 i.e.,  $\sim 4$  to 5 times its decay period of 22.3 years) and can be considered as being stratigraphically  
485 undisturbed. Significant  $^{210}\text{Pb}_{\text{ex}}$  activity in sandy sediments indicates that high clay content is also  
486 not necessary for this method to be used. However, without clay-normalized absorbed  $^{210}\text{Pb}_{\text{ex}}$   
487 activity and without using a model of  $^{210}\text{Pb}$  input during floods, this approach is not sufficiently  
488 accurate for dating episodic sediment accumulation on terraces (Aalto and Nittrouer, 2013).

489 Ages for modern flood deposits have been correctly assigned with the use of lead generated by  
490 mining activity. The latest sediment deposit GE20 (2002) presents EF of lead similar to those of  
491 1969. This latest sedimentary deposit (GE20) might reflect remobilization of ancient floodplain  
492 sediments, acting as a secondary contamination source during large flood events. However, the  
493 similarity of EF values in the 2002 flood deposit and in current stream sediments (E. Resongles,

494 HSM, personal communication, 2014), rather points out limited improvement of sediment quality  
495 by waste water treatment over recent years. Interestingly, the values of EF of Pb in units GG3 and  
496 GG4 (1958 and 2002 events in cave GG) are the same that in the equivalent flood event in the  
497 sequence GE16 and GE20 (1958 and 2002 events in terrace GE). This would suggest that each  
498 flood event is characterized by an EF of Pb. This result also means that the EF ratio of Pb is not  
499 controlled by the particle size distribution. If this is confirmed in later studies, EF of Pb could be  
500 used as another proxy for dating flood deposits in this study area.

501 Eighty percent of dates on charcoal samples are much older than is reasonably expected (Fig. 7).  
502 In the GE terrace, the prevailing inversion of dates, with many of these recording ages older than  
503 expected, is most likely a response to remobilization of sediment. The Gardon River does not  
504 transport material downslope in direct fashion from upstream source areas to our study site  
505 during a single, rapid flood event, but rather in a process that comprises several episodic floods,  
506 small channel migration events on the Gard plain between the Alès graben and Gardon gorges is  
507 envisioned. During extreme flood events, the inundated area is considerably increased and may  
508 cover a part of the old terraces. Sediment is temporarily stored until it is exposed by small  
509 channel migration or erosion of old terraces, mobilized and then once again redeposited. Other  
510 processes may affect the radiocarbon dating techniques on charcoals such as alteration of  
511 samples, by percolation, infiltration from underlying sections (Evans, 1985; Tornqvist et al.,  
512 1998), or hardwater effect (a term for the old-carbon reservoir derived from dissolved carbonate  
513 rocks; Saarnisto, 1988). Sediments of large flood deposits in GE and GG contain a high  
514 proportion of quartz, (>45%), illite/mica (>45%), and relatively little carbonate or dolomite  
515 (<3%). These minerals present in flood deposits derive mainly from the erosion of Paleozoic  
516 granite, schist, and gneiss rocks in the upper part of the Gardon drainage basin. Charcoals have  
517 probably the same origin, i.e., coming from the combustion of trees that initially lived in the

518 Cévennes Mountains. Thus, consistent with the origin of the sediment, our radiocarbon dates do  
519 not have a significant hardwater error, i.e., not initially affected by an oldcarbon reservoir.  
520 Another possible explanation lies in the industrial past of the study area. The Gardon watershed  
521 presents numerous coal mines, which were extensively exploited during the nineteenth and  
522 twentieth centuries. The sediment of terrace GE contains a high proportion of small graphite  
523 particles (~ 80% of the carbon material in the different flood units sieved). Therefore, it can also  
524 be suggested that the binding of small particles of dead carbon on the charcoal produce an aging  
525 of the  $^{14}\text{C}$  ages. We estimated the induced aging process by adding 10% of a dead carbon on a  
526 charcoal dated to 1950. Ten percent is a relatively high value. In this case, this charcoal would  
527 have an age of 1079 years AD ( $1950 - t_{\text{modern } ^{14}\text{C with 10\% of dead carbon}} = 1950 - \ln(100/90) * 8266.6$ ),  
528 which cannot explain the results of the radiocarbon dating on charcoals. To conclude, all these  
529 other processes alone may not account for the extremely wide range in age offset and chronologic  
530 error; and the remobilization of sediment is probably the first process, which can affect our  
531 radiocarbon dates.

532 Radiocarbon dating on seeds seems to give better results. Almost two reasons may explain this  
533 dating difference between charcoal and seeds. Firstly, the seed is an annual product of a living  
534 plant when charcoal is produced by incomplete combustion of a living or dead tree/shrub,  
535 possibly very old. This effect is called 'inbuilt age' or 'old wood effect' (Gavin, 2001) because  
536 woody plants maintain old tissues in their structure; branches and stems could be greatly older  
537 than the date of the fire event and even more than the flood event. Thus the  $^{14}\text{C}$  date of a charcoal  
538 might be significantly older than a  $^{14}\text{C}$  date of a seed in the same flood unit. Secondly, charcoals  
539 are relatively large and decay-resistant, they are likely to remain in the vicinity of the riverbank a  
540 longer time than smaller and more readily decomposed seeds (Oswald et al., 2005). At site GE,  
541 the seeds probably have a local origin. The identified seeds are essentially *Polycnemon*, *Carex*,



542 *Sambucus ebulus*, and *Medicago*, which grow presently on the riverbank. However, although  
543 dating of seeds provides better results than charcoal, the accuracy of this technique is limited  
544 because of the large uncertainty of the  $^{14}\text{C}$  dates compared to discrete flood events. Only the  
545 combined use of  $^{210}\text{Pb}$ ,  $^{137}\text{Cs}$  and geochemical analysis of mining-contaminated sediments with  
546 the instrumental flood record can be applied to discriminate and date the recent slackwater  
547 deposits of the terrace GE and cave GG.

548

#### 549 *6.2. Uncertainties affecting record completeness*

550 The principal goal of a typical slackwater paleoflood investigation is to enumerate floods  
551 represented in the stratigraphic record as accurately and completely as possible and to determine  
552 their timing as precisely as possible (Kochel and Baker, 1988). This task is influenced by several  
553 types of uncertainty, which include the effects of stratigraphic ambiguity, erosion, internal  
554 stratigraphic complexity, incomplete exposure, pedogenesis, stratigraphic record self-censoring  
555 (House et al., 2002), and the uncertainties for dating slackwater flood sediments. Taking into  
556 account these effects have important implications for evaluating the information content of  
557 regional or site-specific fluvial paleoflood data. The stratigraphic records of GE and GG are  
558 excellent examples to illustrate the effects of erosion/preservation in a context of a progressively  
559 self-censoring vertically accreting sequence. The sedimentary flood record between 1958 and  
560 2010 at site GE seems complete. Prior to 1958, this record is incomplete, as indicated by the fact  
561 that fewer post-pollution flood units (seven units) are preserved than there were flood events with  
562 a discharge of sufficient magnitude to cover the sedimentary surface (25 events approximately).  
563 As suggested, the most likely cause of this incomplete record is erosion. The second largest flood  
564 on record was that of 1958; however, the stratigraphy suggests that this event was not responsible  
565 for the erosion of earlier deposits. The contact between units GE15 and GE16 is characterized by

566 buried soils, and no evidence of an erosive contact is observed. It is likely, therefore, that the  
567 sedimentary record reflects a change in preservation potential of the sediments as distinct from  
568 the erosive capability of a particular flood. During the 78-year period 1880-1958, 25 floods of a  
569 sufficient magnitude ( $> 1450 \text{ m}^3/\text{s}$ ) have covered the terrace. Since 1958, however, the frequency  
570 of inundation of the deposits has been lower, there have only been five or six floods in 52 years  
571 large enough to exceed the necessary threshold discharge ( $> 1700 \text{ m}^3/\text{s}$ ). The progressive increase  
572 of threshold discharge and the reduced frequency of inundation at the terrace could allow  
573 stabilisation of the vegetation cover and improved protection against erosion from subsequent  
574 large magnitude flood events (the extreme 2002 event has not eroded the buried soils of the 1976  
575 event). A high frequency of events would not have enabled such a high degree of stabilisation,  
576 rendering the deposits more susceptible to erosion. In cave GG located 15 m above the channel  
577 bed, the sedimentary flood record between 1907 and 2010 seems complete, as indicated by the  
578 fact that there are as many post-pollution flood units (three units) preserved as flood events with a  
579 discharge of sufficient magnitude to cover the sedimentary surface (three events: 1907, 1958, and  
580 2002). Here, the low frequency of events would have enabled a high degree of stabilisation of the  
581 sedimentary flood record, rendering the deposits less susceptible to erosion. This higher  
582 stabilisation is also probably facilitated by a strong decrease of the flood current velocity in this  
583 cave. To conclude, at low elevation sites, frequent flooding may erode the slackwater flood  
584 sediments (e.g., the lower part of terrace GE). In contrast, deposits in high elevation caves or  
585 terraces (largest floods) may have a larger preservation potential, since only extreme events are  
586 able to flush away the sediments accumulated at these higher sites. These observations are not  
587 new. They have been stated previously in the paleoflood literature with varying degrees of  
588 emphasis (House et al., 2002; Thorndycraft et al., 2005a,b). However, our study in the Gardon  
589 River illuminated several types of uncertainties and suggested several others with an excellent

590 example to illustrate the effects of erosion/preservation in a context of a progressively self-  
591 censoring, vertically accreting sequence.

592

### 593 *6.3. Relation to other paleoflood records in the region*

594

595 Sheffer et al. (2008) described a series of 10 distinct slackwater deposits in a cave 12 m above the  
596 river bed (cave GH) at 400 m downstream of the GE site. From this cave, Sheffer et al. (2008)  
597 deduced an increase of flood events during the Little Ice Age and to a cold and wet phase around  
598 2850 years ago. This is an important result because it allowed us to highlight a link between flood  
599 events and climate variability at the regional and southern European scale. Cave GH is located at  
600 an elevation below the 2002 flood water level representing low magnitude floods, and slackwater  
601 deposits matched a minimum associated discharge of 2600 m<sup>3</sup>/s. Cave GH contains at least  
602 seven units deposited in the last 2000 years (Sheffer et al., 2008). Assuming a minimum discharge  
603 of 2600 m<sup>3</sup>/s, the upper part of this cave should record at least eight flood events during the  
604 twentieth century and not only seven during the last 2000 years. This discrepancy could be related  
605 to erosion because of the low position of the cave or to erroneous radiocarbon dates. As observed  
606 in terrace GE where 80% of dates on charcoal samples are much older than is reasonably  
607 expected, radiocarbon ages on charcoal samples of slackwater deposits in cave GH could also be  
608 erroneous in the uppermost part of this cave. To conclude, a supplementary geochronological  
609 study of this alluvial sequence would be necessary to confirm or not these first  
610 palaeohydrological results of Sheffer et al. (2008).

611

612

613

## 614 **8. Conclusion**

615 Our detailed paleoflood investigation on the Gardon River has shown some strengths and  
616 weaknesses of slackwater paleoflood hydrology as a technique for improving understanding of  
617 the frequency of floods in bedrock channels.  $^{210}\text{Pb}$ ,  $^{137}\text{Cs}$ , and geochemical analysis of mining-  
618 contaminated sediments have been used to reconstruct the history of slackwater flood deposits.  
619 This approach was combined with the continuous record of Gardon water levels since 1890 to  
620 assign ages to slackwater deposits. At cave GG and fluvial terrace GE, respectively located at 15  
621 and 10 m above the channel bed, these dating techniques have been successfully applied and  
622 illustrate the potential of this multidating approach in dating recent slackwater flood deposits.  
623 The sedimentary flood record was complete in cave GG but not in terrace GE. We deduced that  
624 at low elevation sites, frequent flooding could erode the slackwater flood sediments (e.g., the  
625 lower part of terrace GE). In contrast, deposits in high elevation caves or terraces (largest floods)  
626 could have a larger preservation potential, as only extreme events were able to flush away the  
627 sediments accumulated at these higher sites.

628 Most  $^{14}\text{C}$  dates on wood charcoal samples (80%) in the terrace GE were much older than the age  
629 reasonably expected. In the terrace, the prevailing inversion of dates, with so many of these  
630 recording ages older than expected, was most likely a clear response to fluvial remobilization of  
631 sediment and their organic contents. Radiocarbon dating on seeds seems to give better results and  
632 could be explained by an absence of 'inbuilt age' effect and low decay-resistance compared to  
633 wood charcoals. However, although the dating of seeds provides better results than wood  
634 charcoal, the accuracy of this technique is limited to date flood events from the most recent  
635 centuries. Only the combined use of  $^{210}\text{Pb}$ ,  $^{137}\text{Cs}$ , and geochemical analysis of mining-

636 contaminated sediments with the instrumental flood record can be applied to discriminate and  
637 date the recent slackwater deposits of the terrace GE and cave GG.

638

## 639 **Acknowledgements**

640

641 This project was totally funded by the ANR commission (EXTRAFLO project). The authors wish  
642 to thank Thierry Montecinos, Marie Bouchet, Stéphanie Garnero, Isabelle Avril, Cyril Soustelle,  
643 Neri for their help in fieldwork; the IRSTEA team for doing bathymetric cross sections; the DDE  
644 Nîmes for the historical flood data; Laurent Bouby for seeds identifications. We thank the  
645 Laboratoire de Mesure  $^{14}\text{C}$  (LMC14) ARTEMIS in the CEA Institute at Saclay (French Atomic  
646 Energy Commission) for the  $^{14}\text{C}$  analyses (EXTRAFLO project). We thank the three anonymous  
647 reviewers for their constructive comments on the manuscript.

648

## 649 **References**

650

- 651 Aalto, R., Nitttrouer, C., 2012.  $^{210}\text{Pb}$  geochronology of flood events in large tropical river  
652 systems. (2012). *Phil. Trans. R. Soc. A* 370, 2040–2074.
- 653 Appleby, P. G., Oldfield, F., 1978. The calculation of  $\text{Pb-210}$  dates assuming a constant rate of  
654 supply of unsupported  $\text{Pb-210}$  to the sediment. *Catena* 5, 1–8.
- 655 Appleby, P., Oldfield, F., 1992. Application of lead-210 to sedimentation studies. In: Ivanovich,  
656 M., Harmon, R.S., (Eds.), *Uranium Series Disequilibrium, Application to Earth, Marine and*  
657 *Environmental Sciences*. Clarendon Press, Oxford, UK, pp. 773–778.
- 658 Atwater, B.F., Trumm, D.A., Tinsley, J.D., III, Stein, R.S., Tucker, A.B., Donahue, D.J., Jull,  
659 A.J.T., Payen, L.A. 1990. Alluvial plains and earthquake recurrence at the Coalinga  
660 anticline. In Rymer, M.J., Ellsworth, W.L. (Eds.), *The Coalinga, California, Earthquake of*  
661 *May 2, 1983*. Publisher City, ST, pp. 273-297, 1487.
- 662 Baker, V.R., 1987. Paleoflood hydrology and extraordinary flood events. *Journal of Hydrology*

- 663 96, 79–99.
- 664 Baker, V.R., Kochel, R.C., 1988. Flood sedimentation in bedrock fluvial systems. In: Baker,  
665 V.R., Kochel, R.C., Patton, P.C. (Eds.), *Flood Geomorphology*. Wiley, city,USA, pp. 123–  
666 137.
- 667 Baker, V.R., Webb, R.H., House, P.K., 2002. The scientific and societal value of paleoflood  
668 hydrology. In: House, P.K., Webb, R.H., Baker, V.R., Levish, D.R. (Eds.), *Ancient Floods,  
669 Modern Hazards: Principles and Applications of Paleoflood Hydrology*. Water Science and  
670 Application Series, vol. 5, AGU, Washington, DC, pp. 127– 146.
- 671 Benito, G., Sopena, A., Sanchez, Y., Machado, M.J., Perez Gonzalez, A., 2003a. Palaeoflood  
672 record of the Tagus River (central Spain) during the late Pleistocene and Holocene.  
673 *Quaternary Science Reviews* 22, 1737–1756.
- 674 Benito, G., Sanchez-Moya, Y., Sopena, A., 2003b. Sedimentology of high-stage flood deposits of  
675 the Tagus River, central Spain. *Sedimentary Geology* 157, 107–132.
- 676 Benito, G., Lang, M., Barriendos, M., Llasat, M.C., Frances, F., Ouarda, T., Thorndycraft, V.R.,  
677 Enzel, Y., Bardossy, A., Coeur, D., Bobee, B., 2004. Use of systematic, palaeoflood and  
678 historical data for the improvement of flood risk estimation. Review of scientific methods.  
679 *Nat. Hazards* 31, 623–643.
- 680 Benito, G., Thorndycraft, V.R., 2005. Palaeoflood hydrology and its role in applied hydrological  
681 sciences. *Journal of Hydrology* 313, 3–15.
- 682 Bonnifait, L., Delrieu, G., Le Lay, M., Boudevillain, B., Masson, A., Belleudy, P., Gaume E.,  
683 Saulnier, G.-M., 2009. Hydrologic and hydraulic distributed modelling with radar rainfall  
684 input: reconstruction of the 8-9 September 2002 catastrophic flood event in the Gard region,  
685 France. *Advances in Water Resources* 32, 1077–1089.
- 686 Bonté, P., Ballais, J.L., Masson, M., Ben Kehia, H., Eyraud, C., Garry, G., Ghram, A., 2001.  
687 Datations au  $^{137}\text{Cs}$ ,  $^{134}\text{Cs}$  et  $^{210}\text{Pb}$  de dépôts de crues du XXe siècle. *Datation, XXIe  
688 rencontres internationales d'archéologie et d'histoire d'Antibes*, Ed. APDCA, 141–157.
- 689 Cremers, A., Elsen, A., De Preter, P., Maes, A. 1988. Quantitative analysis of radiocaesium  
690 retention in soils. *Nature* 335, 247–249.
- 691 Davies, B.E., Lewin, J., 1974. Chronosequences in alluvial soils with special reference to historic  
692 lead pollution in Cardiganshire, Wales. *Environ Pollut* 6, 49–57.
- 693 DREAL, 2008. Internet site: <http://basol.developpement-durable.gouv.fr/>

- 694 El kadi Abderrezzak, K., Paquier, A., 2009. One-dimensional numerical modeling of sediment  
695 transport and bed deformation in open channels. *Water Resour. Res.* 45, W05404.
- 696 Elbaz-Poulichet, F., Bruneel, O., Casiot, C., 2006. The Carnoules mine. Generation of As-rich  
697 acid mine drainage, natural attenuation processes and solutions for passive in-situ  
698 remediation. *Documentation IRD*, p 1–8.
- 699 Ely, L.L., Baker, V.R., 1985. Reconstructing paleoflood hydrology with slackwater deposits  
700 Verde River, Arizona. *Physical Geography* 6, 103–126.
- 701 Ely, L.L., Webb, R.H., Enzel, Y., 1992. Accuracy of post-bomb  $^{137}\text{Cs}$  and  $^{14}\text{C}$  in dating fluvial  
702 deposits. *Quaternary Research* 38, 196–204.
- 703 Enzel, Y., Ely, L.L., Martinez, J., Vivian, R.G., 1994. Paleofloods comparable in magnitude to  
704 the catastrophic 1989 dam failure flood on the Virgin River, Utah and Arizona. *Journal of*  
705 *Hydrology* 153, 291–317.
- 706 Evans, L.J., 1985. Dating methods of Pleistocene deposits and their problems. VII. Paleosols.  
707 In:ed. Rutter, N.W. (Ed.), *Dating Methods of Pleistocene Deposits and Their Problems*. Repr.  
708 Ser. Geosci. Canada, Toronto, Canada, pp. 53–59.
- 709 Gavin, D.G., 2001. Estimation of inbuilt age in radiocarbon ages of soil charcoal for fire history  
710 studies. *Radiocarbon* 43, 27–44.
- 711 Golberg E., 1963. Geochronology with  $^{210}\text{Pb}$ . *Radioactive Dating*. International Atomic  
712 Energy Agency, Vienna, Austria, pp. 121–31.
- 713 He, Q., Walling, D.E., 1996. Interpreting particle size effects in the adsorption of  $^{137}\text{Cs}$  and  
714 unsupported  $^{210}\text{Pb}$  by mineral soils and sediments. *J. Environ. Radioact* 30, 117–137.
- 715 Hindel, R., Schlich, J., De Vos, W., Ebbing, J., Swennen, R., Van Keer, Y., 1996. Vertical  
716 distribution of elements in overbank sediment profiles from Belgium, Germany and The  
717 Netherlands. *Journal of Geochemical Exploration* 56, 105–122.
- 718 House, P.K., Pearthree, P.A., Klawon, J. E., 2002. Historical Flood and Paleoflood Chronology  
719 of the Lower Verde River, Arizona: Stratigraphic Evidence and Related Uncertainties. In :  
720 House, P. K., Webb, R. H., Baker, V. R., Levish D. R., (Eds.), *Ancient Floods, Modern*  
721 *Hazards*, American Geophysical Union, Washington, D.C., pp. 267–293.
- 722 Huet, P.X., Martin, J.L., Prime, P., Foin, C., Laurain, P., Cannard, 2003. Retour d'expérience  
723 décrues de septembre 2002 dans les départements du Gard, de l'Hérault, du Vaucluse, des  
724 Bouches du Rhône, de l'Ardeche et de la Drome. *Rapport de l'Inspection Générale de*

- 725 l'Environnement. Ministre de l'Ecologie et du D'Developpement Durable, République  
726 Française. 133 pp. Available at the Internet site:  
727 <http://www.environnement.gouv.fr/infoprat/Publications/publi-ige.htm>.
- 728 Knox, J.C., Daniels, J.M., 2002. Watershed scale and the stratigraphic record of large floods. In :  
729 House, P. K., Webb,R. H., Baker, V. R., LevishD. R., (Eds.), *Ancient Floods, Modern*  
730 *Hazards*, American Geophysical Union, Washington, D.C., pp. 237–255.
- 731 Kochel, R.C., Baker, V.R., Patton, P.C., 1982. Palaeohydrology of southwest Texas. *Water*  
732 *Resour. Res.* 18, 1165–1183.
- 733 Kochel, R.C., Baker, V.R., 1988. Paleoflood analysis using slack water deposits. In: Baker, V.R.,  
734 Kochel, R.C., Patton, P.C. (Eds.), *Flood Geomorphology*. John Wiley and Sons, U.S.A., pp.  
735 357–376.
- 736 Lewin, J., Davies, B.E., Wolfenden, P.J.,1977. Interaction between channel change and historic  
737 mining sediments. In K.J. Gregory (Ed.), *River channel changes*, pp. 353–367.
- 738 McHenry, J.R., Ritchie, J.C., 1977. Physical and chemical parameters affecting transport of  
739  $^{137}\text{Cs}$  in arid watersheds. *Water Resources Research* 13, 923–927.
- 740 Nuissier, O., Ducrocq, V., Ricard, D. , Lebeau-pin, C. , Anquetin, S. , 2008. A numerical study of  
741 three catastrophic precipitating events over southern France. I : Numerical framework and  
742 synoptic ingredients. *Quart. J. Roy. Meteor. Soc.*134, 111–130.
- 743 Nydal, R., Lovseth, K., 1983. Tracing bomb  $^{14}\text{C}$  in the atmosphere 1%2-1980. *Journal of*  
744 *Geophysical Research* 88, 3621–3642.
- 745 Oswald, W.W., Anderson, P.M., Brown, T.A., Brubaker, L.B., Hu, F.S., Lozhkin, A.V., Tinner,  
746 W., Kaltenrieder, P., 2005. Effects of sample mass and macrofossil type on radiocarbon  
747 dating of arctic and boreal lake sediments. *The Holocene* 15, 758–767.
- 748 Popp, C. J., Hawley, J. W., Love, D. W., Dehn, M., 1988. Use of radiometric ( $^{137}\text{Cs}$ ,  $^{210}\text{Pb}$ ),  
749 geomorphic, and stratigraphic techniques to date recent oxbow sediments in the Rio Puerto  
750 Drainage. Grants Uranium Region, New Mexico. *EnvironmentalGeology and Water Science*  
751 3, 253–269.
- 752 Ritchie, J.C., McHenry, J.R., Gil, A.C., 1974. Fallout  $^{137}\text{Cs}$  in the soils of three small  
753 watersheds. *Ecology* 55, 887–890.
- 754 Saarnisto, M., 1988. Time-scales and dating. In: Huntley, B., WebbIII III, T. (Eds.), *Vegetation*  
755 *History*. Handbook of vegetation science. Kluwer Academic Publishers, Dordrecht, pp. 77–



- 756 112.
- 757 SAGE des Gardons, 2000. Annexe 1 au Schéma d'Aménagement et de Gestion des Eaux des  
758 gardons, SAGE, pp 187.
- 759 Sheffer, N.A., Rico, M., Enzel, Y., Benito, G., Grodek, T., 2008. The palaeoflood record of the  
760 Gardon River, France: A comparison with the extreme 2002 flood event. *Geomorphology* 98,  
761 71–83.
- 762 Springer, G.S., 2002. Caves and their potential use in paleoflood studies. In: House, P.K., Webb,  
763 R.H., Baker, V.R., Levish, D.R. (Eds.), *Ancient Floods, Modern Hazards: Principles and*  
764 *Applications of Paleoflood Hydrology*. Water Science and Applications, AGU, pp. 329–344.
- 765 Stokes, S., Walling, D.E., 2003. Radiogenic and isotopic methods for the direct dating of fluvial  
766 sediments. In: Kondolf, M., Piegay, H. (Eds.), *Tools in Fluvial Geomorphology*. Wiley,  
767 Chichester, pp. 233–267.
- 768 Stuiver, M., Reimer, P.J.. 1993. Extended 14C data base and revised CALIB 3.0 14C age  
769 calibration program. *Radiocarbon* 35, 1, 215–30.
- 770 Sutherland, R.A., 1989. Quantification of accelerated soil erosion using the environmental tracer  
771 Caesium-137. *Land Degradation and Rehabilitation* 1, 199–208.
- 772 Thorndycraft, V.R., Benito, G., Rico, M., Sopena, A., Sánchez-Moya, Y., Casas-Planes, A.,  
773 2004a. A Late Holocene Paleoflood record from slackwater flood deposits of the Llobregat  
774 River, NE Spain. *Journal Geological Society of India* 64 (4), 549–559.
- 775 Thorndycraft, V., Brown, A.G. , Pirrie, D., 2004b. Alluvial records of Medieval and prehistoric  
776 tin mining on Dartmoor, SW England. *Geoarchaeology*, 19, 219–236.
- 777 Thorndycraft, V., Benito, G., Rico, M., Sopena, A., Sánchez-Moya, Y., Casas, A., 2005a.  
778 Paleoflood hydrology of the Llobregat River, NE Spain: a 3000year record of extreme  
779 floods. *Journal of Hydrology* 313 (1-2), 16–31.
- 780 Thorndycraft, V.R., Benito, G., Walling, D.E., Sopena, A., Sanchez-Moya, Y., Rico, M., Casas,  
781 A., 2005b. Caesium-137 dating applied to slackwater flood deposits of the Llobregat River,  
782 N.E. Spain. *Catena* 59, 305–318.
- 783 Tisnérat-Laborde, N., Poupeau, J.J., Tannau, J.F., Paterne, M., 2001. Development of a  
784 semiautomated system for routine preparation of carbonate samples. *Radiocarbon* 43, 299–  
785 304.
- 786 Tornqvist, T.E., Van Ree, M.H.M., Van't Veer R., Van Geel B., 1998. Improving methodology

787 for high-resolution reconstruction of sealevel rise and neo-tectonics and paleoecological  
788 analysis and AMS 14C dating of basal peats. *Quat. Res.* 49, 72–85  
789 Trumbore, S.E., 2000. Radiocarbon geochronology. In: Noller, J.S., Sowers, J.M., Lettis, W.R.  
790 (Eds.), *Quaternary Geochronology: Methods and Applications*. AGU, Washington, D.C., pp.  
791 41–60.  
792 Walling, D.E., He, Q., 1997. Use of fallout 137Cs in investigations of overbank sediment  
793 deposition on river floodplains. *Catena* 29, 263–282.  
794 Webb, R.H., Jarrett, R.D., 2002. One-dimensional estimation techniques for discharges of  
795 paleofloods and historical floods. In: House, P.K., Weeb, R.H., Baker, V.R., Levish, D.R.  
796 (Eds.), *Ancient Floods, Modern Hazards: Principles and Applications of Paleoflood*  
797 *Hydrology*. Water Resources Monograph, vol. 5. AGU, Washington, D.C., pp. 111–12.

798

799

800

801

802

### 803 **List of figures and table**

804

805 Fig. 1: Topography, hydography, and geological maps of the Gardon river watershed.

806

807 Fig. 2: Annual maximum gage height available at Remoulins between 1890 and 2010.

808

809 Fig. 3: (A) A map showing the study sites in the Gardon Gorges. (B) Terrace (GE) and cave  
810 (GG), sites of slackwater flood sediment archives .

811

812 Fig. 4 (A) Cross sections of the paleosites used in the model; (B) Calculated stage-discharge  
813 relationships and their envelope and (C) Historical flood series at Remoulins.

814

815 Fig. 5. The proposed chronology for the terrace GE slackwater flood deposits,  $d_{50}$ ,  $^{137}\text{Cs}$   
816 activities,  $^{210}\text{Pb}_{\text{ex}}$  activities, EF of lead, the peak annual instantaneous discharges series at  
817 Remoulins. The envelope on the range of discharges at Remoulins that may have submerged the  
818 site resulting from the sensitivity analysis is shown. The individual slackwater flood units  
819 deposited by a particular event are annotated.

820

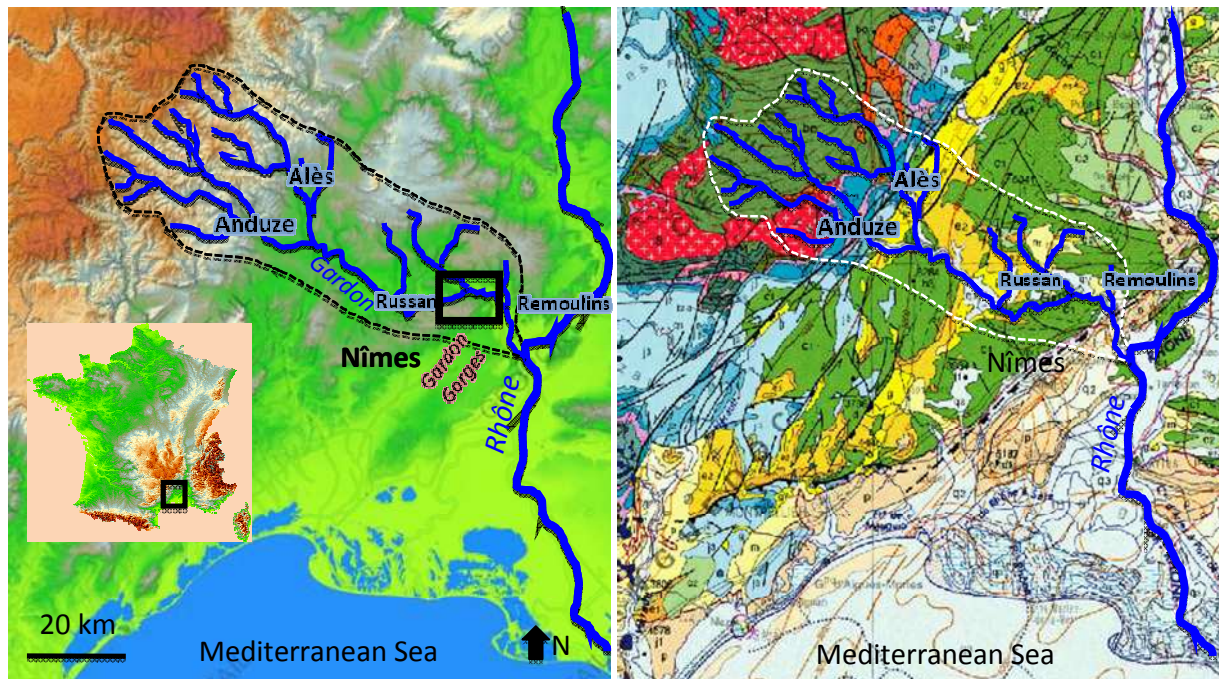
821 Fig. 6. The proposed chronology for the cave GG slackwater flood deposits,  $d_{50}$ ,  $^{137}\text{Cs}$  activities,  
822  $^{210}\text{Pb}_{\text{ex}}$  activities, the peak annual instantaneous discharges series at Remoulins. The envelope on  
823 the range of discharges at Remoulins that may have submerged the site resulting from the  
824 sensitivity analysis is shown. The individual slackwater flood units deposited by a particular  
825 event are annotated.

826

827 Fig. 7. Stratigraphy and age model of site GE. Radiocarbon ages on wood charcoals (in blue) and  
828 seeds (in red) in BP and calendar ages ( $2\sigma$ )

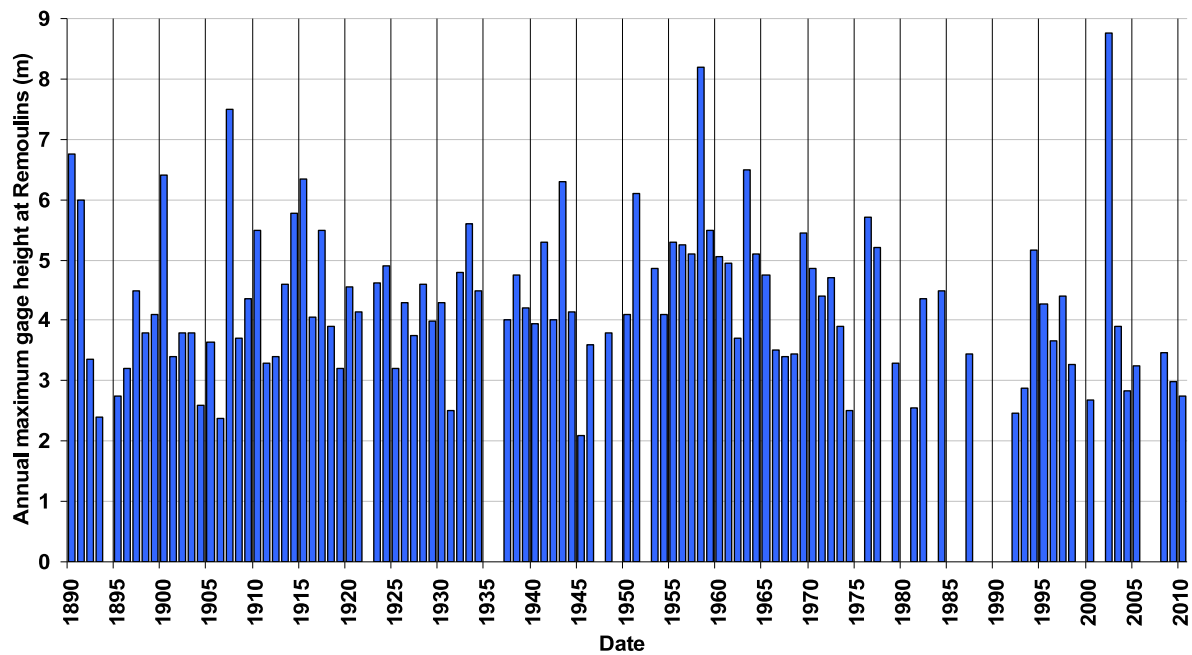
829

830 Table 1. Results from radiocarbon dating. All calibrated ages were calculated within  $2\sigma$ .  
831 Calibration was carried out using CALIB 6.1.0. The age model integrates the minimum and the  
832 maximum value of the calibrated age.



833

834 Fig. 1: Topography, hydrography, and geological maps of the Gardon river watershed.



835  
836  
837

Fig. 2: Annual maximum gage height available at Remoulins between 1890 and 2010.

(A)



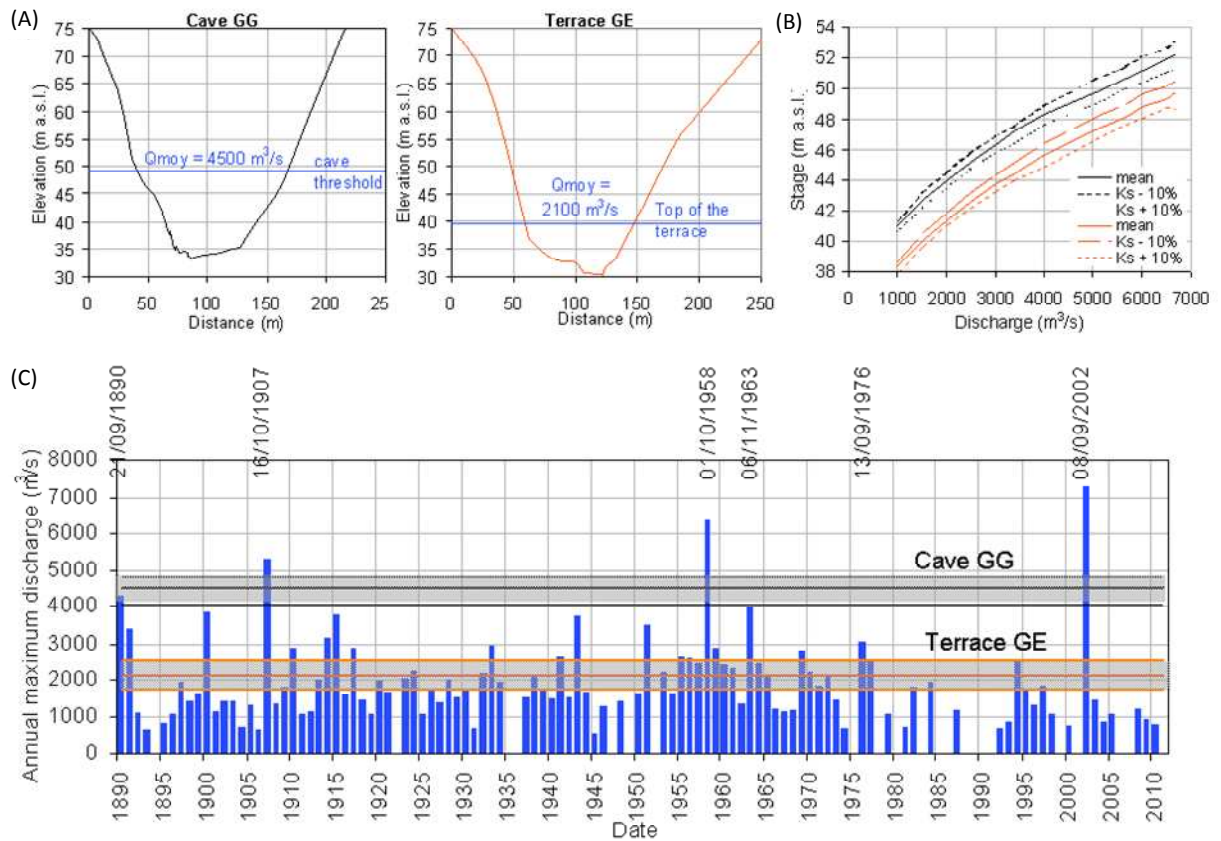
(B)



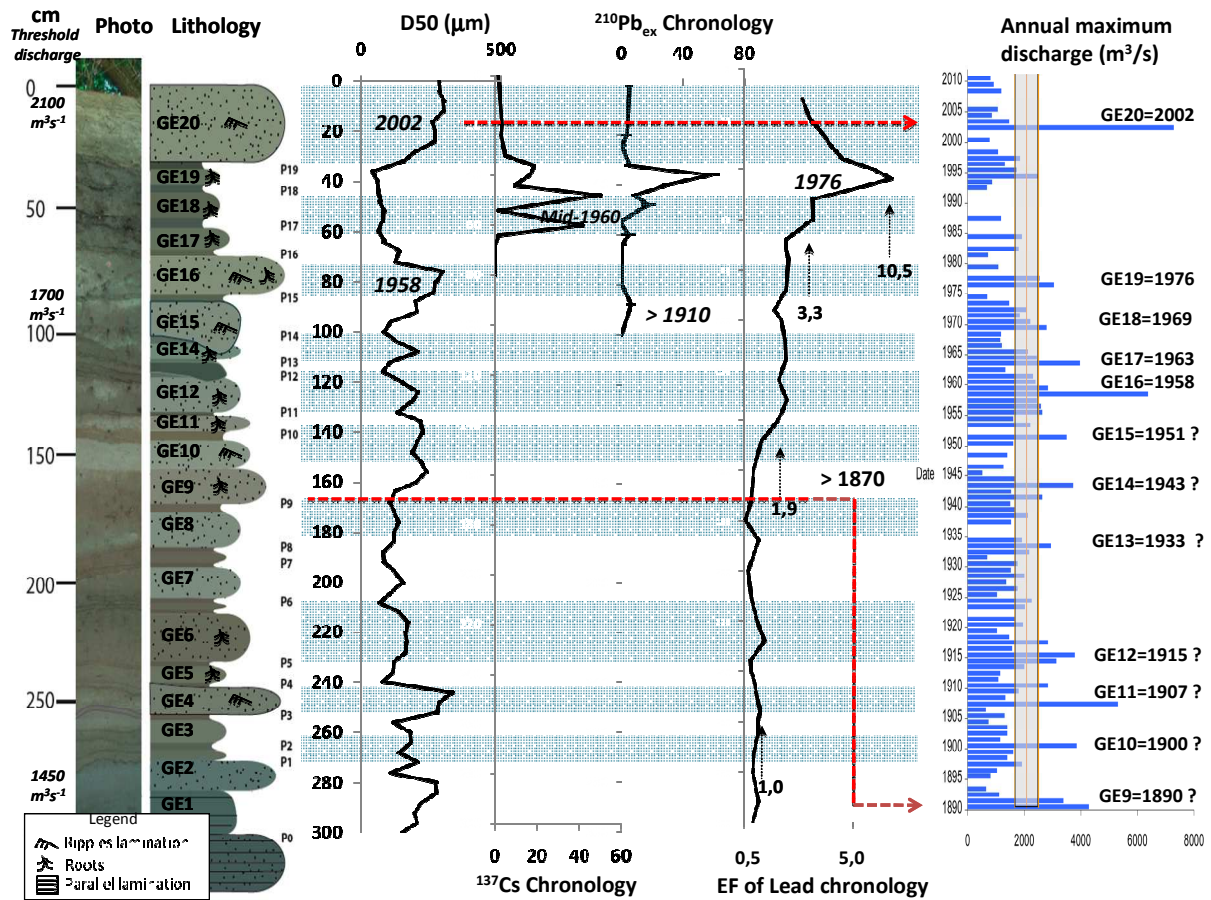
838

839 Fig. 3: (A) A map showing the study sites in the Gardon Gorges. (B) Terrace (GE) and cave

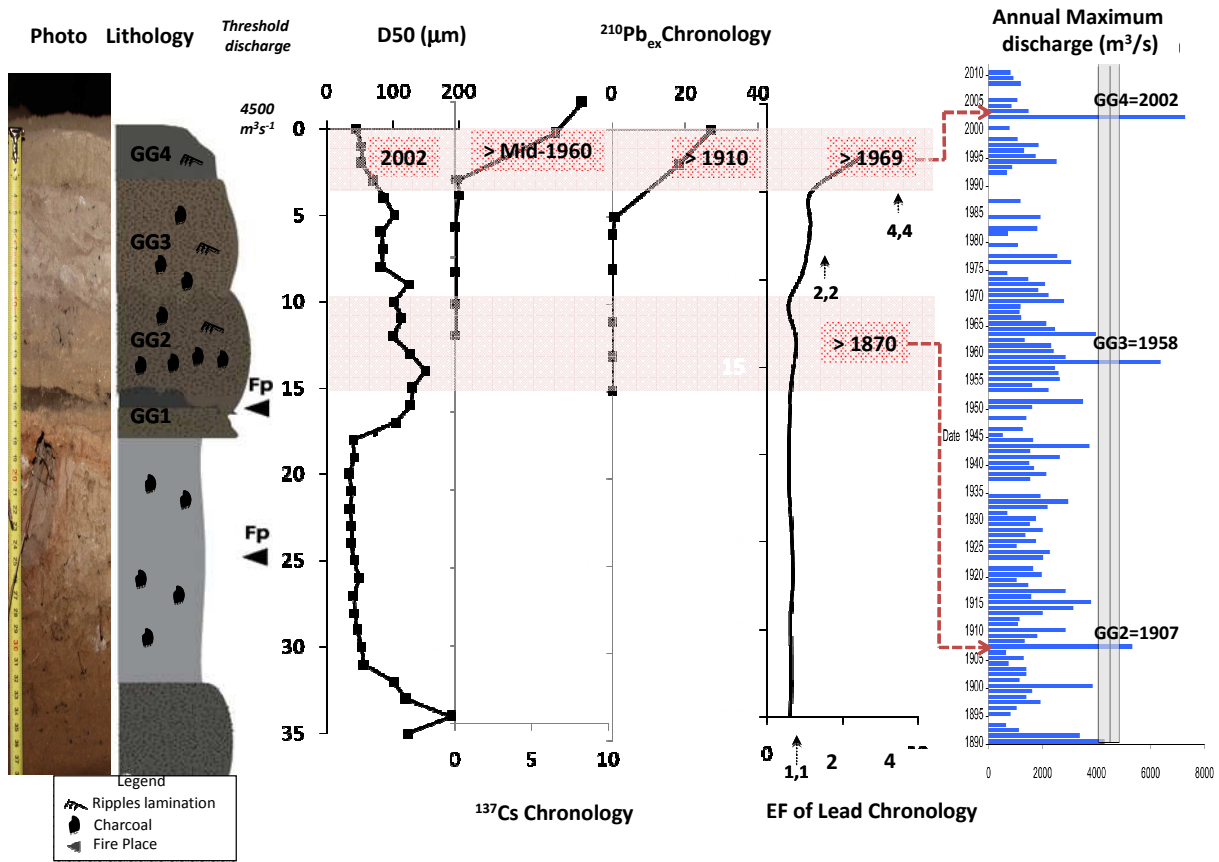
840 (GG), sites of slackwater flood sediment archives .



841 Fig. 4 (A) Cross sections of the paleosites used in the model; (B) Calculated stage-discharge  
842 relationships and their envelope and (C) Historical flood series at Remoulins.

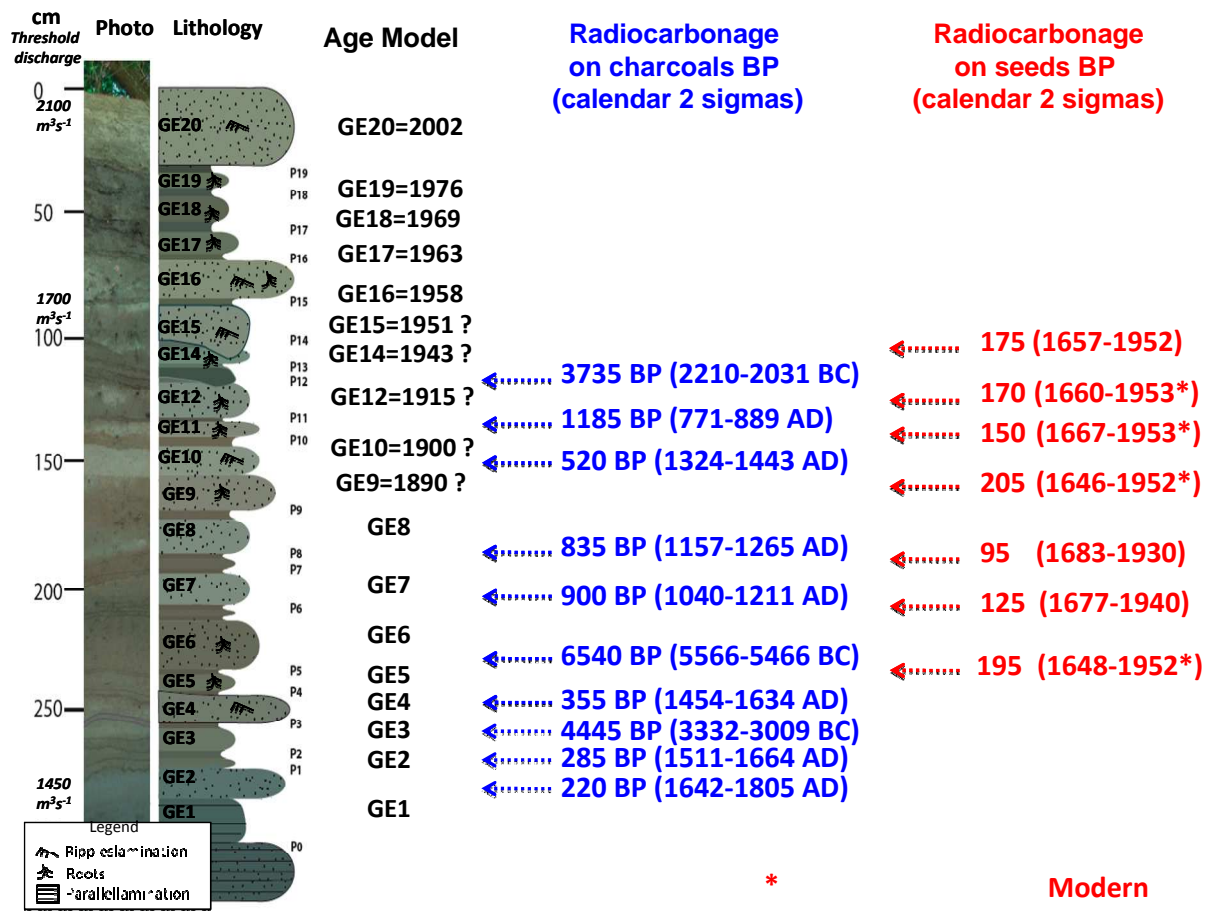


843 Fig. 5. The proposed chronology for the terrace GE slackwater flood deposits, d50, <sup>137</sup>Cs  
 844 activities, <sup>210</sup>Pb<sub>ex</sub> activities, EF of lead, the peak annual instantaneous discharges series at  
 845 Remoulins. The envelope on the range of discharges at Remoulins that may have submerged the  
 846 site resulting from the sensitivity analysis is shown. The individual slackwater flood units  
 847 deposited by a particular event are annotated.



848 Fig. 6. The proposed chronology for the cave GG slackwater flood deposits, d50,  $^{137}Cs$  activities,  
 849  $^{210}Pb_{ex}$  activities, the peak annual instantaneous discharges series at Remoulins. The envelope on  
 850 the range of discharges at Remoulins that may have submerged the site resulting from the  
 851 sensitivity analysis is shown. The individual slackwater flood units deposited by a particular  
 852 event are annotated.





853

854 Fig. 7. Stratigraphy and age model of site GE. Radiocarbon ages on wood charcoals (in blue) and  
 855 seeds (in red) in BP and calendar ages ( $2\sigma$ )

856

857 Table 1. Results from radiocarbon dating. All calibrated ages were calculated within  $2\sigma$ .  
 858 Calibration was carried out using CALIB 6.1.0. The age model integrates the minimum and the  
 859 maximum value of the calibrated age.

Sample	Type	Age	Calibrated age (agreement % Age model)	
GE113-116	charcoal	3735±35	2210-2031 BC (94%)	2210-2031 BC
GE 132-135	charcoal	1185±30	771-899 AD (92%)	771-899 AD
GE 148-152	charcoal	520±30	1324 1345 AD (10%) 1393-1443 AD (89%)	1324-1443 AD
GE 192-195	charcoal	835±30	1157-1265 AD (100%)	1157-1265 AD
GE 208-214	charcoal	900±30	1040-1110 AD (44%) 1115-1211 AD (55%)	1040-1211 AD
GE 238-243	charcoal	6540±40	5566-5466 BC (92%)	5566-5466 BC
GE 257-262	charcoal	355±35	1454-1529 AD (47%) 1540-1634 AD (53%)	1454-1634 AD
GE 267-270	charcoal	4445±35	3332-3213 BC (38%) 3132-3009 BC (51%)	3332-3009 BC
GE 275-280	charcoal	285±35	1511-1601 AD (61%) 1616-1664 AD (37%)	1511-1664 AD
GE 283-289	charcoal	220±30	1642-1683 AD (39%) 1735-1805 AD(48%)	1642-1805 AD
GE 103-107	seed	175±30	1657-1696 AD (19%) 1725-1814 AD (55%) 1917-1952* AD (20%)	1657-1952*AD
GE 122-127	seed	170±30	1660-1698 AD (18%) 1722-1817 AD (54%) 1916-1953* AD (20%)	1660-1953* AD
GE 138-142	seed	150±30	1667-1708 AD (17%) 1718-1783 AD (33%) 1796-1827 AD (12%) 1831-1889 AD (19%) 1910-1953* AD (19%)	1667-1953* AD
GE 157-161	seed	205±30	1646-1685 AD (29%) 1732-1808 AD (55%) 1928-1952* AD (16%)	1646-1952* AD
GE 188-193	seed	95±30	1683-1735 AD (28%) 1805-1930 AD (71%)	1683-1930 AD
GE 207-212	seed	125±30	1677-1766 AD (35%) 1800-1895 AD (47%) 1903-1940 AD (16%)	1677-1940 AD
GE 233-238	seed	195±30	1648-1691 AD (25%) 1729-1811 AD (57%) 1922-1952* AD (20%)	1648-1952*AD

860